

Chapter

An Application of Bio-Inspired Superwetting Surfaces: Water Collection

Chang Li, Zhongshi Ni and Ying Li

Abstract

On a superwetting surface, droplet behaviour can be manipulated. Utilising the directional motion and coalescence of water, water collection (including fog harvesting) is a significant application of superwetting surfaces. In the plant and animal kingdom, many biological surfaces show excellent water-collecting function. This chapter summarises the development and recent progress of the natural and bio-inspired surfaces that can collect water. The biomimetic models, i.e., the model of spider silks, cactus, and desert beetles are introduced. The corresponding mechanism, raw materials or approaches to mimic natural surfaces and optimised structures which show improved water-collecting performance are explained. Future directions for the water-collecting material are forecasted.

Keywords: super-wetting surface, bio-inspired, water transport, spider silk, cactus, desert beetle

1. Introduction

Water plays a crucial role in most creatures alive in nature, covering requests for organismic daily consumptions, agricultural irrigation, and industrial production. Water shortage is an acute problem in many areas of the world. Collecting water with satisfactory efficiency from a humid/foggy atmosphere is deemed as a fundamental step to release the tough issue, which is also a hot and significant research direction.

In water collection, fog-water capturing and water droplet transport for collection are two main steps. A single superhydrophilic or superhydrophobic surface could not meanwhile accelerate both courses. For example, hydrophilicity can speed up fog-water capturing. However, it may cause water retention, which may slow down water transport and further water harvesting. On a hydrophobic surface, droplets can roll easily for collection while the efficiency of fog-water capturing is very low. To handle the dilemma, researchers have paid attention to the natural superwetting surfaces which have an exciting ability to manipulate liquid behaviours [1, 2]. They possess special wettability designs or/and unique micro/nano-structures.

Creatures surviving in droughty environments usually have a special ability to collect water. For example, some desert plants and animals can capture water from the humid air during nightfall caused of temperature differences. Creatures living in

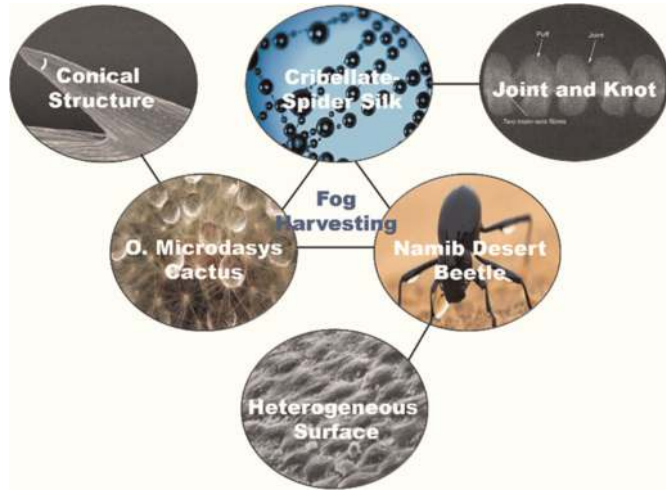


Figure 1. Biological surface that can collect water: spider silk with joint and knot, cactus with conical structure, desert beetle with heterogeneous surface.

highly humid environments also have the ability to manipulate water droplets or flow. For example, on spider silk, morning dews are spontaneously collected. This chapter will respectively introduce the water collection ability of spider silks, cactus, and desert beetles (**Figure 1**). The natural surface and bio-inspired model to mimic the surface structure are involved. The strategies to enhance water collecting efficiency by designing special wettability or micro/nano-structure are detailly introduced.

2. Spider silks inspired spindle-knot fibre

2.1 Biological model and theoretical analysis of spindle-knot fibre

The ability to harvest fog is determined by the fog-water catching performance at the surface together with the removal efficiency of the captured water from the surface [3, 4]. One-dimensional (1D) fog collectors usually make use of some hydrophilic composition or/and water-loving structure to rapidly seize the water from a humid environment. Subsequently, small droplets hang on the 1D material and accumulated into larger droplets gradually. Finally, large droplets can fall into a container due to growing gravity.

Spider web has been well-known for its excellent mechanical, biochemical and pharmaceutical properties because of its network structure and the composition of biological proteins [5–8]. In the recent decade, a single spider silk was deeply studied and has been deemed as a perfect model for designing artificial water collector. The periodic spindle-knot structure on spider silk (similar to bead-on-string fibre) is useful. This structure can give rise to driving forces on dew based on Laplace pressure difference and probable surface energy gradient. These forces drive the droplet moving to the spindle knot, where the combined droplet is released and collected [9]. The Laplace pressure difference (**Figure 2(a)**) can be calculated by the following formula,

$$F_L \sim \gamma \left(\frac{1}{R_1'} - \frac{1}{R_2'} \right) \frac{\sin \beta}{R_1 - R_2} V \quad (1)$$

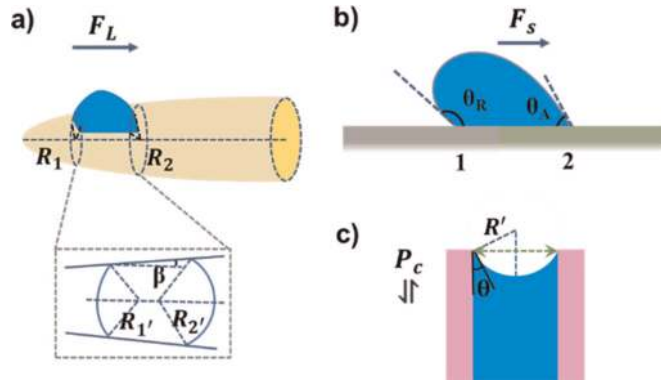


Figure 2.
 Sketch of force analysis on the bio-inspired water-collecting units.

where γ is the surface tension of water droplet, R_1' and R_2' indicates the local curvatures of the contact lines at two opposite sides of droplet along the spindle knot, R_1 and R_2 indicate the local radius of the spindle knot. Angle β is the half apex angle of the knot, which is related to the size and shape of the knot. V is volume of water droplet on knot, which can be approximate estimated by the formula $V = \pi R_0^3 / 12$, where R_0 indicates the radius of the droplet.

The spindle knot usually had a higher axial-parallel roughness than the other area on the fibre, contributing to a smaller contact angle. Therefore, the spindle knot is more hydrophilic and has a higher surface energy. The consequent driving force resulting from surface energy gradient (**Figure 2(b)**) can be described as follow,

$$F_S = \int_{L_j}^{L_k} \gamma (\cos \theta_A - \cos \theta_R) dl \quad (2)$$

where θ_A and θ_R , respectively indicate the advancing and receding angle of the water droplet on spider silk, and dl is the integrating variable from original silk joint (L_j) to the spindle knot (L_k).

Capillary pressure (result from small holes or probable grooves on spindle-knot) gradient can also be introduced into this system to speed up the water combination or transportation rate. The capillary force P_c (**Figure 2(c)**) is estimated by the Young–Laplace formula [10],

$$P_c = 2\gamma / R' \quad (3)$$

where R' indicates the curvature radius of surface of water in small holes or grooves.

2.2 Featured structures made by multi-methods using various materials

When aiming at mimicking the biological spindle-knot structure (**Figure 3(a)**) with consequent water-collecting function, diverse biomimetic methods are employed. For example, dip-coating, electro-dynamic, fluid-coating, and microfluidics have been developed or utilised [8, 16]. As shown in **Figure 3(b–j)**, diverse spindle-knot structures can be prepared.

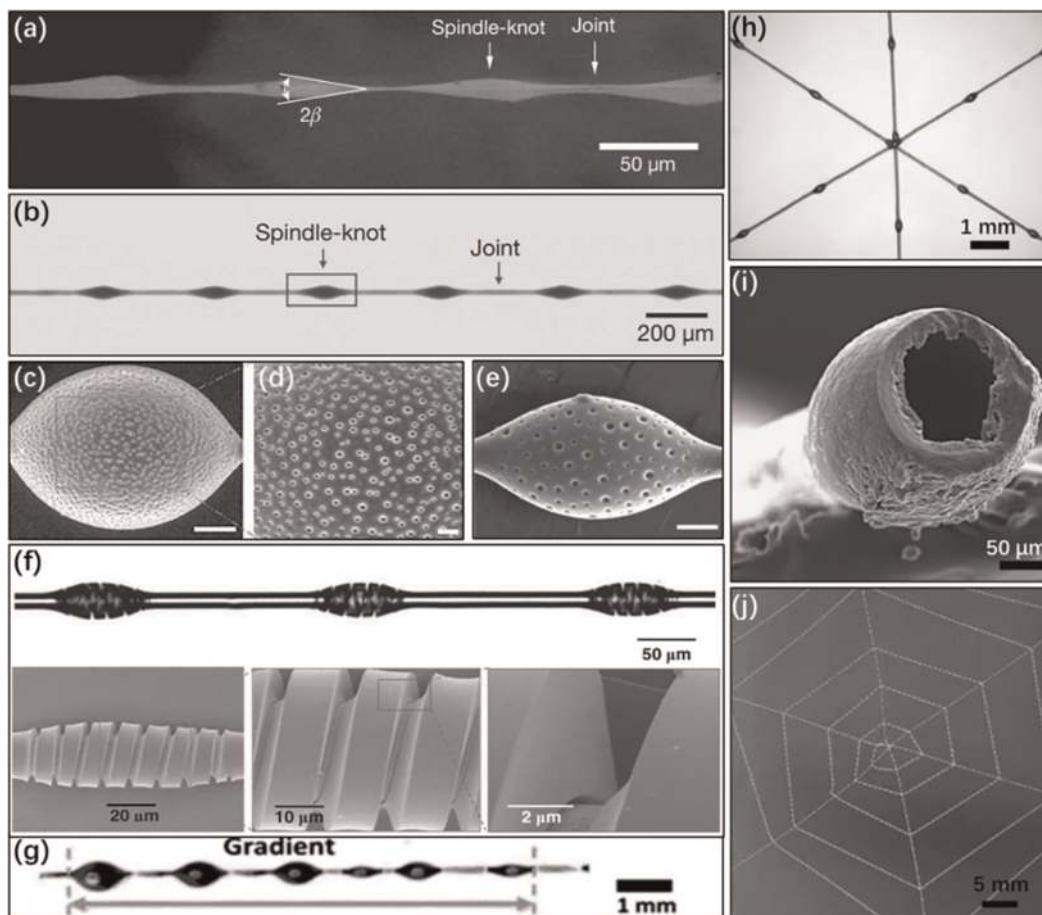


Figure 3. Spider silk and diverse artificial spider silks. (a) SEM image of spider silk in nature [9], scale bar 50 μm . (b) Optical image of artificial spider silk via traditional dip-coating [7], scale bar 200 μm . (c, d) SEM images of micro-porous bead on string fibre via dip-coating with breath figure method [11], scale bar 10 μm . (e) SEM images of gradient-porous bead on string fibre via dip-coating with breath figure method [11], scale bar 10 μm . (f) Optical image and SEM images of helical spindle-knot fibre via deep-coating and sequent calcination [12], scale bar 50 μm . (g) optical image of a gradient-sized spindle knot fibre via fluid-coating at an increasing drawn-out rate [13], scale bar 1 mm. (h) Photo of magnetic assembly integrated artificial spider silks [14], scale bar 1 mm. (i) SEM image of hollow artificial spider silk via microfluidics using nitrogen as inconsecutive phase [15], scale bar 50 μm . (j) Photo of integrated topological artificial spider silk to mimic spider web [15], scale bar 5 mm.

2.2.1 Dip-coating

Dip-coating is the earliest-developed, frequently-used, convenient and mature approach to mimic spider silk with fog harvest ability. In a typical process, a Nylon fibre (usually 50 ~ 300 μm in diameter) was immersed deeply into a polymer solution which had been prepared in advance. Afterwards, it was drawn out horizontally and a tubular membrane composed of the polymer solution wrapped the fibre uniformly. The membrane broke up into several ellipsoids on account of Rayleigh instability and then turned into a periodic spindle knot on fibre while getting dried (**Figure 3(b)**).

According to the Eqs. (1) and (2) mentioned above, the actuating force for droplet directional transportation depends on the shape and size of the spindle knots together with the interval of each two periodic knots. These factors can be optimised by changing the processing parameters such as the viscosity or volatility of polymer solution, drawn-out velocity, and desiccation condition [17].

In order to improve fog-water capturing efficiency, the spindle knot can be further designed and manufactured into a porous spindle knot due to the high specific surface area and enhanced absorbability. For example, breath-figure method [11, 18] was utilised to achieve steerable micro-pores (**Figure 3(c and d)**), and gradient pores (**Figure 3(e)**).

Some spindle knot with ring or helical grooves (**Figure 3(f)**) which show better performance has been developed [12]. To fabricate such periodic ring or helical grooves spindle knot on 1D material, an added procedure of calcination or desiccation under a high temperature (more than 800 K) was essential. Conventional polymer fibres such as Nylon could not stay non-deformation or unshrink at such high temperature. Hence, Glass Fibre or Carbon Fibre (usually 7–15 μm in diameter), with greater high-temperature resistance properties and other mechanical performance, were employed as host fibre material in these studies [11, 12]. Furthermore, rather than the organic polymer solution, some inorganic compounds and materials with ameliorate biocompatibility, such as Titanium salt/oxide [12, 19], would be used if environment conservation or other intention was taken into consideration.

2.2.2 Fluid-coating

Dip-coating is capable of fabricating fine accurate structure (usually 7 ~ 300 μm diameter fibre with minimum feature size about 5 μm) on the fibre. However, it is difficult for dip-coating to realise large scale preparation. Fluid-coating was developed and continuously massive coating comes true [20]. Artificial spider silks in random length are likely to be synthesised via this approach, which is a promising method for the industry.

The principle and operating steps of fluid-coating to prepare spindle knot are similar to dip-coating. As is reported in previous work [21], a Nylon fibre (about 70 μm in diameter) was steadily fastened in a polymer solution reservoir (width: 2 cm, length: 3.5 cm, height: 3 cm, with one edge attached to a motor) through two capillary tubes (400 μm inner diameters). The motor drew the fibre out at the desired speed and the polymer solution (parallel to the solution in dip-coating method, **Table 1**) moved with the fibre thanks to the viscous force. Then the fluid covered the fibre to become a cannular polymer membrane and it broke up into droplets on account of Rayleigh instability, which ultimately turned into periodic spindle knots on fibres after evaporation.

The unique feature of fluid-coating lies in the alterable and steerable drawn-out rate. It is reported that by drawing out at a monotone increasing velocity, gradient in thickness of polymer film emerged and gradient-size spindle knots (**Figure 3(g)**) were generated on fibre eventually [13]. Researchers also tried fishing-line fibres, copper fibres and carbon fibres to be the host fibres (**Table 1**) and obtained a satisfactory mechanical property.

2.2.3 Electrodynamic

Electrodynamic technology is another strategy for large-scale preparation of artificial spider silks. This method is good at preparing slender (200 nm ~ 12 μm in diameter) silk with fat spindle or even ellipsoid knot (usually 3 ~ 6 times of the slender silk in diameter, the whole artificial silk namely bead-on-string fibre).

Pervious works [22–24] justified the practicability of a coaxial electrospinning method (namely core-shell electrospinning), which developed from conventional

Ref.	Method	Host fibre	Polymer solution	Structural feature
[9, 17]	DC	Nylon	DMF, PMMA	First-made and similar to real spider silk
[11]	DC	Carbon fibre	DETA, ER	Different porous structure on knot
[12]	DC	Glass fibre	TiBO-P123 sol gel	Helical crack on spindle knot
[21]	FC	Nylon	DMF, PVDF	Surface with different roughness
[21]	FC	Fish-line fibre	DMF, PMMA	Gradient-sized spindle knot
[21]	FC	Copper fibre	DMF, PMMA	Gradient-sized spindle knot

DMF: *N, N*-dimethyl formamide, PMMA: polymethyl methacrylate, PVDF: polyvinylidene fluoride, DMAc: *N, N*-dimethyl acetamide, DETA: Diethylenetriamine, ER: Epoxy resin-44, TiBO: titania butoxide, P123: HO(CH₂CH₂O)₂₀(CH₂CH(CH₃)O)₇₀(CH₂CH₂O)₂₀H.

Table 1.

Materials and polymer solutions are used in dip-coating (DC) and fluid-coating (FC) to make artificial spider silk.

Ref.	Outer fluid (shell)		Inner fluid (core)	
	Solution (wt)	Solvent (w/w)	Solution (wt)	Solvent (vol/vol)
[27]	20% PEG	1:1 MC and DMF	35% Polystyrene	DMF
[28]	25% PMMA	7:3 THF and DMF	30% Polystyrene	DMF
[29]	10% PNIPAM	1:1 THF and DMF	16% PVDF	3:2 DMF and Acetone
[30]	PVDF-HSP-FPOSS ^a	1:1 THF and DMAc	PVDF-HSP-FPOSS ^b	1:1 THF and DMAc

^asol-gel: 2 g PVDF-HEP and 1 g FPOSS in 16 mL solvent.

^bsol-gel: 2 g PVDF-HEP and 1 g FPOSS in 32 mL solvent.

PEG: polyethylene glycol, MC: methylene chloride, DMF: *N, N*-dimethyl formamide, PMMA: polymethyl methacrylate, THF: tetrahydrofuran, PNIPAM: poly(*N*-isopropylacrylamide), PVDF: polyvinylidene fluoride, PVDF-HSP-FPOSS: poly(vinylidene fluoride-co-hexafluoropropylene) with fluorinate polyhedral oligomeric silsesquioxane, DMAc: *N, N*-dimethyl acetamide.

Table 2.

Chemical reagents are used for outer and fluid polymer solutions in different electrodynamic studies to make artificial spider silk.

coaxial electrospinning and electrospinning. In this method, heterogeneous liquids with different viscosity and vapour pressure-filled two different channels of jet. Dilute solution in the outer channel was electro-sprayed into micro-particles (finally acting as spindle knots) due to Rayleigh instability (or combined with wet-assembly technique) [19, 25]. The inner viscous liquid channel was electrospun to micro- or nano-fibres [26].

As is displayed in **Table 2**, multifarious chemical substances were used to prepare inner and outer solutions to meet the request for wettability, finance, or environment-protecting [27–30]. To exemplify it, poly-L-lactic acid (PLLA) was chosen as a raw material on the basis of being degradable, whose solution (6 wt% PLLA dissolved in Chloroform and DCM: dichloromethane with different volume rates ranging from 95/5 to 65/35 and stirring at room temperature) electrospun bead-on-string fibre exhibited a higher directional transport performance compared with PVA solution (10 wt% polyvinyl alcohol dissolved in hydrothermal water containing 17 wt% glutaraldehyde) [31].

Albeit electrodynamic approaches can enable relatively large-scale production of bead-on-string hierarchical nanofibres with satisfactory fog-harvesting (normally ~5 g water, fog flow ~25 mL per hour), mechanical properties such as tensile strength should be improved to prolong the lifespan of fibres. To achieve this, adding postprocessing (e.g., carbonation procedures to transfer it into carbon fibre) can be a decent measure.

2.2.4 Microfluidics

Microfluidics was a relatively recent developed technology to continuously fabricate artificial spider silk. By adjusting the relative location of syringe needles in convention microfluidic devices, artificial spider silk could be synthesised via imitating the authentic spinning process of nature spiders [32].

In a coaxial microfluidic device, there are two flows of liquids (**Table 3**) with different feeding rates. In a typical synthesis [33], a micropipette was employed where an Alginate-based composite solution (ABC solution) served as the continuous phase and liquid Paraffin served as the dispersed phase, respectively consisting of the host fibre and spindle-knot of artificial spider silk after dehydration. The diameter of host fibre and geometry size of periodic spindle knot as well as the distance between two adjacent spindle knots can be altered by optimising the parameter of feeding speed of two flows (and their feeding speed ratio).

To achieve the porous surface of joint or spindle-knot of artificial spider silk to get enhanced fog-captured performance, add a component with distinct solubility (salt such as NaCl or CaCl₂) into the liquids and then remove it by washing or soaking in aqueous solution [26]. Analogously, Fe₃O₄ nanoparticles can be added to the volatile oil drops during microfluidic operation to obtain magnetic property of spindle knot. The synthetic 1D materials can then be assembled or patterned (**Figure 3(h)**) into the multidimensional structure under an external magnetic field [14]. Additionally, gas (e.g., nitrogen [15]) can be used as a dispersed phase and bioinspired cavity-microfibres (**Figure 3(i and j)**) can be fabricated.

2.3 Water collecting efficiency of artificial spider silks

By optimising the geometry of periodic spindle knots, artificial fibres could show enhanced performance in fog-harvesting tests (**Figure 4**). As is demonstrated in **Figure 4(a)**, five small water drops moved and combined rapidly within 4.39 s on a PMMA spindle-knot Nylon fibre. It is recorded that when the vertical downward fog

Ref.	Continuous phase	Dispersed phase	Feature
[33]	Sodium Alginate	Liquid Paraffin	Improved microfluidics preparation
[14]	Calcium Alginate	Oil drop+ Fe ₃ O ₄ nanoparticles	Magnetic 2D or 3D assembly fibre
[15]	ABC solution ^a	Nitrogen	Hollow fibre (with topological weave) ^b

^aAlginate based composite (other salts) solution.
^bTopological structure by postprocessing.

Table 3.
Substance employed in microfluidics to produce artificial spider silks and their corresponding feature.

flow was ~ 0.75 m/s, the artificial fibre which is 1.5 mm in length could collect 40 nL of water within 12 s in comparison with 17 nL of natural spider silk under a similar circumstance [21].

Distinct types of spindle knot may give rise to different impact on fog-harvesting function. The in-situ observation and optical images of water collecting test on artificial fibre with gradient-size spindle knots (**Figure 4(b)**) showed that droplet coalescence with a special mode could be implemented. Under $\sim 90\%$ humidity using ultrasonic humidifier, 7.35 mm fibre with gradient-size spindle knots was capable of harvesting water at a rate of 509.4 $\mu\text{L/h}$, while 156.7 $\mu\text{L/h}$ of water was collected using similar fibre with uniform sized periodic spindle knots under the same condition [13]. Porous surface morphology also brings in increasing efficiency of water collecting. As illustrated in **Figure 4(c)**, under same $\sim 100\%$ high humidity condition using humidifier, water collecting efficiency had the following rank: gradient porous structured $>$ homogenous porous structured $>$ smooth spindle-knot fibre [11]. Additionally, spindle knots do play a significant role in improving the water-harvesting efficiency (**Figure 4(d)**).

Intersection would gain an easier access to capture and harvest fog-water (**Figure 4(e)**). In an updated research, two intersectional silks (8.25 μL in 60 s) tended to harvest more water than two parallel silks (4.57 μL in 60 s) in 60s under a 0.408 mL/min fog flow. Topological network bioinspired by spider web exhibited

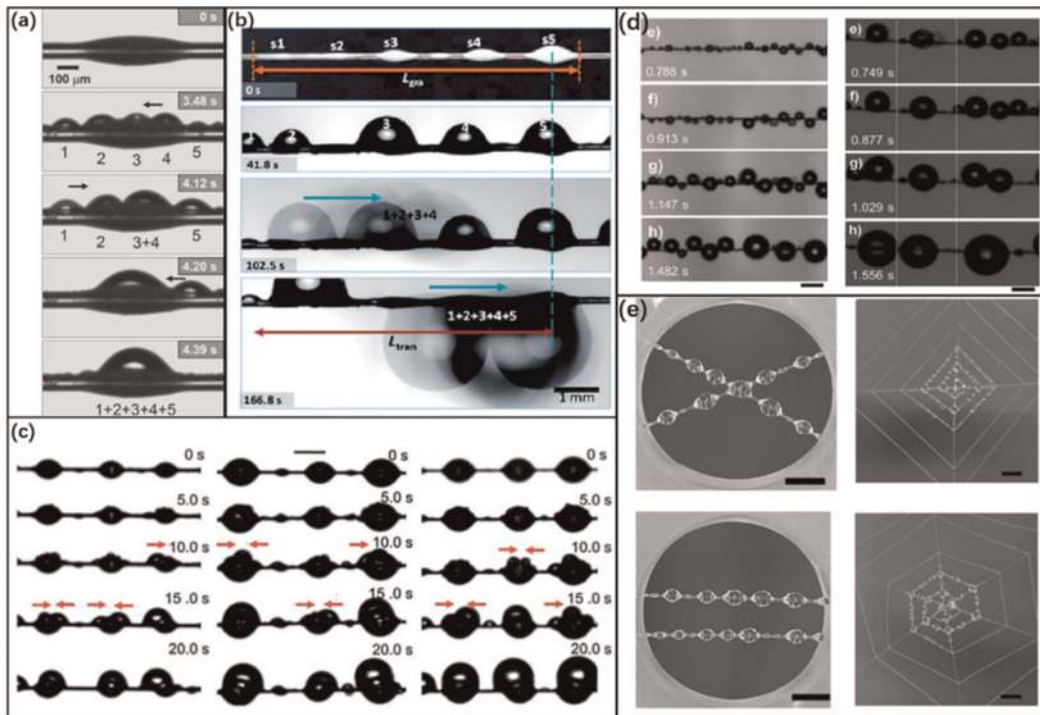


Figure 4. Fog-collecting characterisation images of diverse artificial spider silks. (a) In-situ observation of directional fog harvesting of conventional PMMA spindle-knot (by fluid-coating) on Nylon fibre [21], scale bar 100 μm . (b) Optical images of water collecting on gradient sized PMMA spindle-knot (by fluid-coating) on Nylon fibre [13], scale bar 1 mm. (c) Optical images of aggregation of water droplet of ER knots (all by deep-coating) with smooth, homogenous porous and gradient porous structure on carbon fibres [11], scale bar 50 μm . (d) Optical images of PMMA-PS bead on string (right) fibre and smooth PS (left) fibre (all by electrodynamic) [28], scale bar 20 μm . (e) Photos of fog harvesting on Alginic based cavity (all by microfluids) fibres [15], scale bar 5 mm.

much higher fog-harvesting efficiency: 150 mm topological networks with two radius were able to collect 53.297 μL in 120 s and with three radius, the volume is 68.957 μL in 120 s [15].

By comparing the water collecting performance of diverse artificial spider silks (**Figures 4 and 5**), it can be summarised that appropriate shape (slenderness ratio: 1 ~ 10), size (gradient sized spider-knot) and morphology (knot with porous microstructure especially gradient porous microstructure) of artificial spider silks, resulted from optimised processing parameters (**Figure 5(a)**), will contribute to better fog-harvesting performance. Diverse materials with different structural or wettability design differs in water-harvesting style and efficiency (**Figure 5(b and c)**). Temperature, humidity or flow rate in the water-collecting test may also affect water-collecting volume (**Figure 5(c and d)**).

In addition, 2D or 3D intersectional arrangement of artificial fibre to mimic the real topological spider web in nature turns out to own an larger-scale fog-harvesting capacity than 1D spider silk [4]. For example, combined with advanced multi-directional braiding technology, multidimensional integrated spider silks can be acquired with relatively large scale fog harvesting capacity [34, 35]. These 2D or 3D

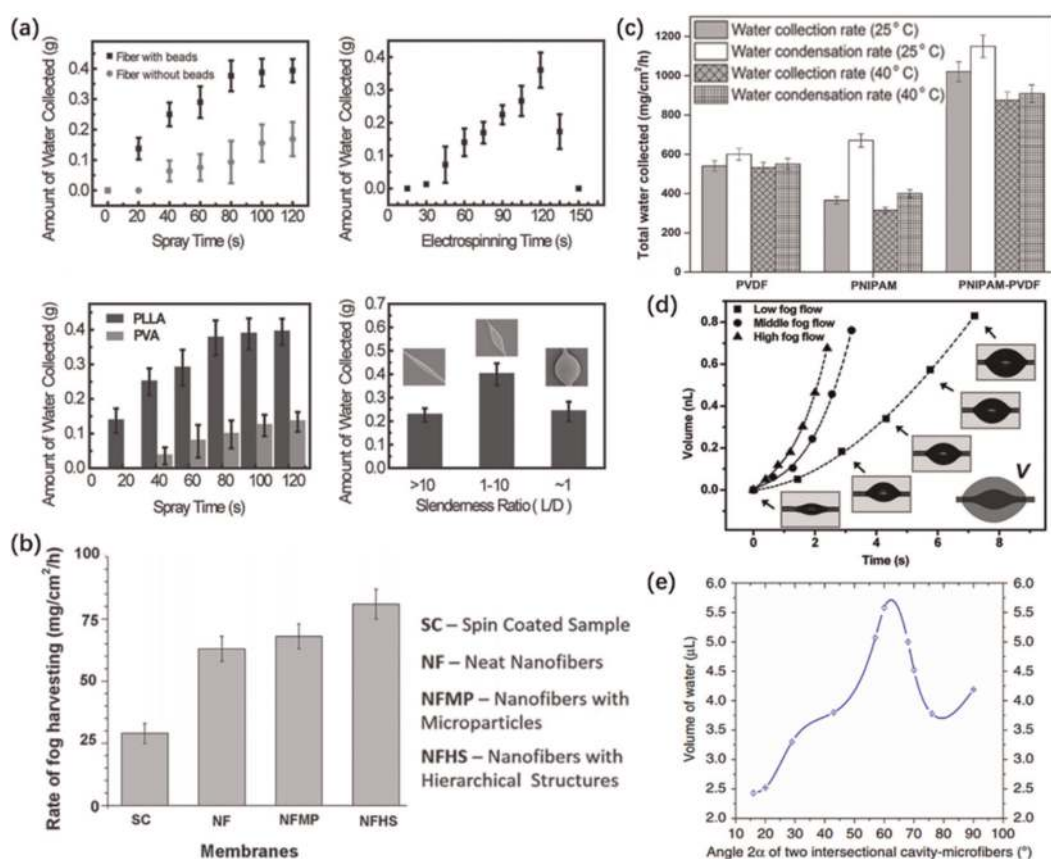


Figure 5. Various factors which may exert influences on fog-harvesting performance of artificial spider silks. (a) Impacts of spray times, electrospinning times in electrodynamic method slenderness ratio, materials and fibre with/without beads on fog-harvesting [31]. (b) Influences of postprocessing and hierarchical structure of fibre on fog-harvesting [30]. (c) Effects of temperature, materials and core-shell structure on water condensation and water harvesting [29]. (d) Impacts of fog flow rate in water-harvesting [17]. (e) Influence of intersectional angle of two artificial spider silk on fog-harvesting [15].

network materials were estimated to harvest up to 0.5 ~ 1.5 ton/day (per square meter of material) fog-water in foggy environment (e.g., industrial cold-water tower). To prepare artificial fibre in industrial scale and to harvest water in much larger scale should be future research topics [36].

3. Cactus inspired conical structure

3.1 Biological model and theoretical analysis of cone

Plants survived in extraordinarily droughty conditions tend to have advanced fog-harvesting ability inevitably. Inspired by a cactus [37], conical structures were developed as a perfect model for water collecting. Agaves [38] and wheat awns [39], which have similar needle-like construction, also can harvest fog. The geometry of cone can be deemed as half of a spindle knot to some degree when analysing driving force. The Laplace force is an attraction to gather fog-water, which can be calculated by Eq. (1). Also, roughness gradient (Eq. (2)) can be introduced.

By integrated the cones into oblique conical micro- and/or nano- array (or barbed array, bioinspired by *Eremopyrum orientale* or ryegrass leaves) [40, 41] on 2D planar materials, anisotropy surface with enhanced water-collecting property from foggy atmosphere were developed. As for the mechanism, oblique array with anisotropy gives rise to a difference in concomitant retention force (F_r) on hindering water transport to two directions. When the droplet moves, the retention force can be estimated by [42]

$$F_r = w\gamma(\cos \theta_{RO} - \cos \theta_{AO}) \quad (4)$$

where w is the width of water droplet, θ_{RO} and θ_{AO} indicate the intrinsic contact angle. Moving along the oblique direction, decreasing solid-liquid contact width is beneficial to postpone the water meniscus resulting in water release, while moving against, increasing solid-liquid contact width causing pinning of water droplet. Experiment also illustrates that the retention forces of the droplet against the oblique direction are larger than those along the oblique direction [40, 43]. As a result, the distinction of retention force along two opposite direction can ultimately lead to water directional removal.

3.2 1D and 2D patterns via different methods using distinct materials

With regards to 1D pattern, research was frequently carried on metals with hydrophilicity. Thanks to the electroconductivity of metals, electrochemical method (e.g., controlled electrochemical corrosion or gradient anodic oxidation) can be employed [44, 45]. For instance, a copper wire (usually ~800 μm in diameter) was placed vertically and attached to the anode of a 10 V DC power with a curled copper sheet connected with the cathode. For one thing, a container filled with CuSO_4 solution (electrolyte) pumps from a syringe pump which increases the liquid level of electrolyte at a constant velocity, causing a gradient of electrochemical corrosion of the copper wire and thus producing a conical shape. For another, controlled by a periodic current (from 0.05 to 0.8 A, pondered for 5 s, and then declined to 0.05 A) using the DC power, the roughness gradient was obtained.

In terms of 2D planar model, an interesting method called soft lithography [40, 41, 44, 45] was developed to directly copy biological surfaces. Primarily, fresh biological sample was fixed flat on a petri dish. Non-fizzy PDMS mixture (10:1 polydimethylsiloxane and its curing agent after uniform stir and vacuum treatment) was decanted into the dish and heated at 325 ~ 353 K for 3 ~ 5 hours (heating temperature and time contributing to hardness and flexibility of as-prepared PDMS model). After free cooling to room temperature, PDMS model was apart from biological sample with caution. Whereupon, the mirror symmetric PDMS mould of target architecture had been prepared. Eventually, an analogous step was repeated to get the target structured model. If the material of target model must be PDMS, original PDMS mirror was fluoridized (fluorination in vacuum at 363 K for 5 h) beforehand. As for PVDF material, PDMS mirror was pressed on the PVDF powders (which has spread on a clean glass slide and heated to 543 K until the organic material were fully melting in advance) at 2×10^6 Pa for 10 seconds. Microstructure of biological sample can be easily copied by such patent. In addition, for conical array surface pattern without using biological sample, the mirror mould mentioned above can also be manufacture via machine spotting, drilling or punching on PE (polyethylene) or PVC (polyvinyl chloride) board [46]. By adding magnetic powders (such as Co) into PDMS before curing, flexible magnetic PDMS pattern was made whose cone array could tilt at desirable angles under controllable external magnetic field [43, 46, 47].

3.3 Fog-harvesting efficiency of cactus inspired structure

Multi-gradient copper wire shows a satisfying efficiency in fog-harvesting tests. As illustrated in **Figure 6(a)**, the first three water drops transported and combined into one droplet within 0.18 s directly the first water drop was formed on the cone copper wire [44]. In another research [45], oxidised copper wire with multi-gradient was compared with the original copper wire, showing a unidirectional movement and enhanced (increasing ~70%, in 60 s) fog harvesting efficiency (**Figure 6(b)**). Fog harvesting performance of such 1D cone sample is associated with the tilt angles of placing sample. As demonstrated in **Figure 6(c)**, the collecting efficiency peaked at 0.36 mg/s (experiment done in temperature 288 K, and fog flow velocity 1.8 m/s) when gradient cone copper wire was placed horizontally [44].

2D biomimetic models also show high efficiency or show larger-scale water-collecting capacity. As demonstrated in **Figure 6(d)**, PDMS surface with vertical needle-like array showed a fog harvesting function at 80% humidity air while magnetic cone with flexibility under alternating magnetic field exhibited 50 times higher fog-harvesting efficiency (at about 0.2 g/h under the quasistatic foggy environment) in 1 hour than the static cone [46]. Biomimetic copied artificial leaf with oblique barbed array on surface involves a fog-harvesting capacity of 95.4 g/m²/h (air flow rate of 10 L/min and 3.5 bar pressure delivering a water nebulization rate of 0.4 mL/min at 296 K) and it was improved to 136.8 g/m²/h after an initiated chemical vapour deposition of hydrophobic surface nanocoating. It is worth noting that by integrated 18 copper wire 1D patterns (fixed on a 6.5 × 6.5 × 0.5 cm Teflon frame, side-to-side horizontally setup) into a tiny water-collecting device, the highest value of fog-harvesting rate can reach up to surprisingly 6180 g/m²/h under 2.4 m/s fog velocity in temperature 288 K [44].

From what is cited above, it is safe to draw a summary that different gradient in surface morphology or shape of cone structure, arrangement of cone or cone array, and wettability of materials will affect fog-harvesting performance.

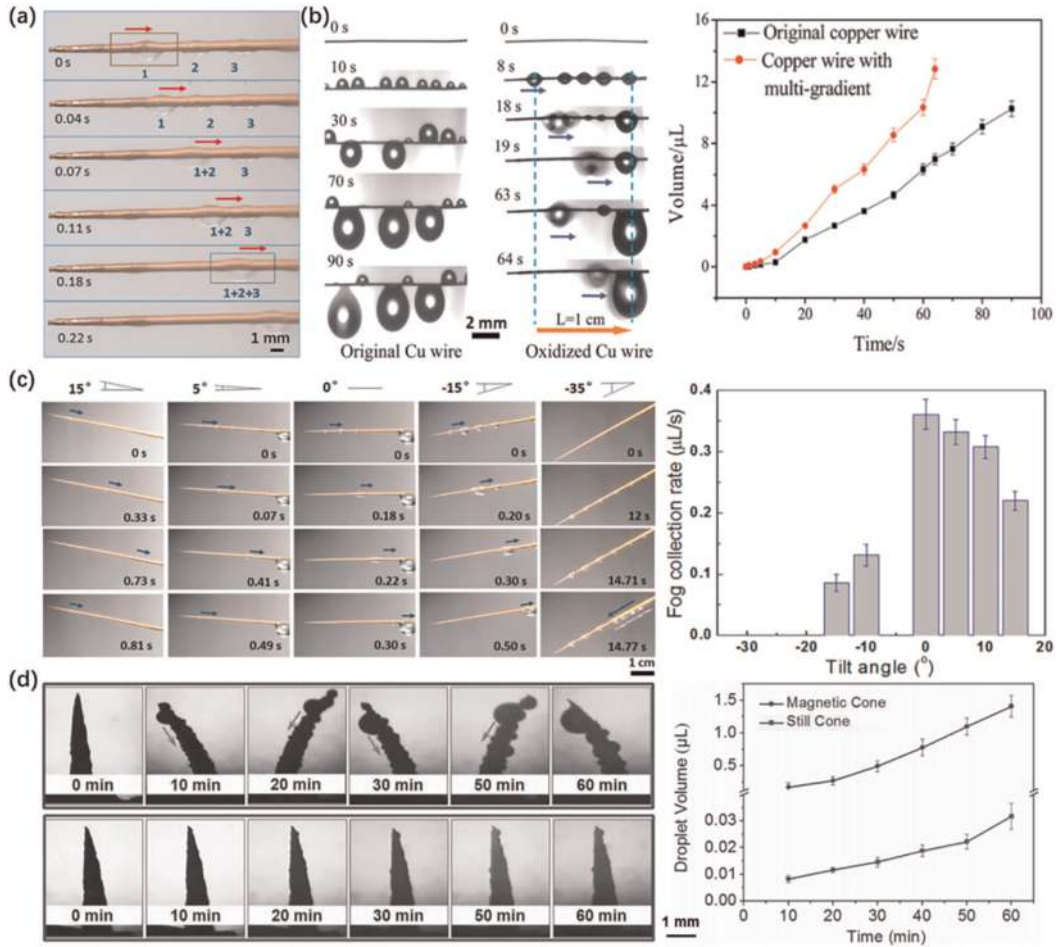


Figure 6. Water-collecting of diverse cone structured patterns. (a) Transport process of first three drops on a multi-gradient cone copper wire (by controlled electrochemical corrosion) [47], scale bar 1 mm. (b) Fog-water collection behaviour between an original copper wire and a multi-gradient cone copper wire (by gradient anodic oxidation) [45], scale bar 2 mm. (c) Fog-water unidirectional transport properties of a multi-gradient cone copper wire (by controlled electrochemical corrosion) at different tilt angles [44]. (d) Water harvesting of a magnetic cone with and without the external magnetic field in the same chamber [41].

4. Desert beetle inspired heterogeneous surface

4.1 Biological model and theoretical analysis of wettability paradox

Namib desert is one of the oldest and driest existing desert in the world. Plenty of species died out while others which have been adapted to the arid conditions (such as Namib desert beetle, spider, snail, grass, cactus) enjoy a good life. Desert beetle, with superhydrophilic wax-free texture (peaks) and hydrophobic wax-coated array (groove) on its back, has long been imitated for fog collecting [48, 49].

Heterogeneous wettability architecture has also been found in the plant kingdom, i.e., the *Salvinia*. *Salvinia* effect [50, 51] represents the stabilisation of an air layer upon a submerged superhydrophobic surface with hydrophilic pins array (which might be a new model for fog-harvesting in the future studies). *Salvinia* wettability paradox further indicates the phenomenon of a functional entirety with discrete wettability, similar to the heterogeneous construction of Namib desert beetle back.

The principle of its fog-harvesting ability is the fact that superhydrophilicity makes it easier to seize water and superhydrophilic texture combined with hydrophobicity groove gives an appointed route for water drop to transport. The discrete driving force of wettability imbalance can be calculated by Eq. (2), further describing as

$$F_w = \gamma(\cos \theta_{\text{hydrophilic}} - \cos \theta_{\text{hydrophobic}}) \quad (5)$$

where $\theta_{\text{hydrophilic}}$ and $\theta_{\text{hydrophobic}}$ are contact angle of water on two opposite sides with two distinct wettability. If the $\theta_{(\text{super})\text{hydrophobic}} > 150^\circ$ and $\theta_{(\text{super})\text{hydrophilic}} < 5^\circ$, a large driving force caused by wettability imbalance will impel water droplet into more hydrophilic region, which can be further designed as fog-harvesting model.

4.2 Various wettability paradox obtained by diverse advanced technology

In order to obtain an entirety with discrete wettability, scientists with distinct research backgrounds may utilise diverse advanced approaches. A facile avenue is to composite (in a macroscopic scale) another material with distinct wettability onto the surface of original material. For example, a superhydrophobic copper oxide gauze can be incorporating onto the surface of a hydrophilic PS flat sheet through thermal pressing [52].

Another strategy is to fabricate by various coating or corrosion technology on a basic material (e.g., glass slide) to selectively change the wettability (e.g., via a mask). For instance, primarily, a superhydrophilic surface composed of TiO₂ nanoparticles was obtained on a bare glass substrate via a spin-coating method. Then, it was superhydrophobically treated using heptadecafluorodecyl-trimethoxysilane (FAS). Last but not least, the functional pattern was realised by illuminating the FAS-modified film under UV light with a photomask. The FAS-treated superhydrophobic TiO₂ surface becomes superhydrophilic again owing to the photocatalytic decomposition of the FAS monolayer after being exposed to UV light [53]. Via this approach, circle-pattern, 4-, 5-, 6-, 8-pointed star-patterns, and other graphic patterns was manufactured on surface (**Figure 7(a)**). The graphic patterns depend on the geometry of photomask.

Laser treatment can be used in manufacturing wettability gradient. For example, a superhydrophilic-superhydrophobic surface on Pyrex wafer was prepared using femtosecond lasers, through the processes of Teflon-like polymer (CF₂)_n depositing and Femtosecond laser ablation to selectively remove the superhydrophobic coating [55]. Similarly, selective plasma corrosion [56], electrochemical etching [57], and inkjet printing [54], with similar designed procedures, have been developed to obtain micropatterns with wettability paradox.

4.3 Fog-harvesting efficiency of bioinspired heterogeneous surface

The strategy of fog-harvesting inspired by desert beetle turns out to be very effective. As is displayed in **Figure 8(a)**, a high-contrast (superhydrophobic array) wetting glass collected more (60%) fog within 30 min than a blank glass [55]. In another research, by changing the size and arrangement density of superhydrophobic array, $\sim 400\%$ improvement in fog-harvesting test (**Figures 7(b) and 8(b)**) was realised (increasing from 149 g/m²/h to 618 g/m²/h, at about 295 K environmental temperature and ~ 0.1 m/s fog rate using humidifier, the surface temperature of sample: 277 K and air around sample: 90–95% humidity, vertically placed) [54].

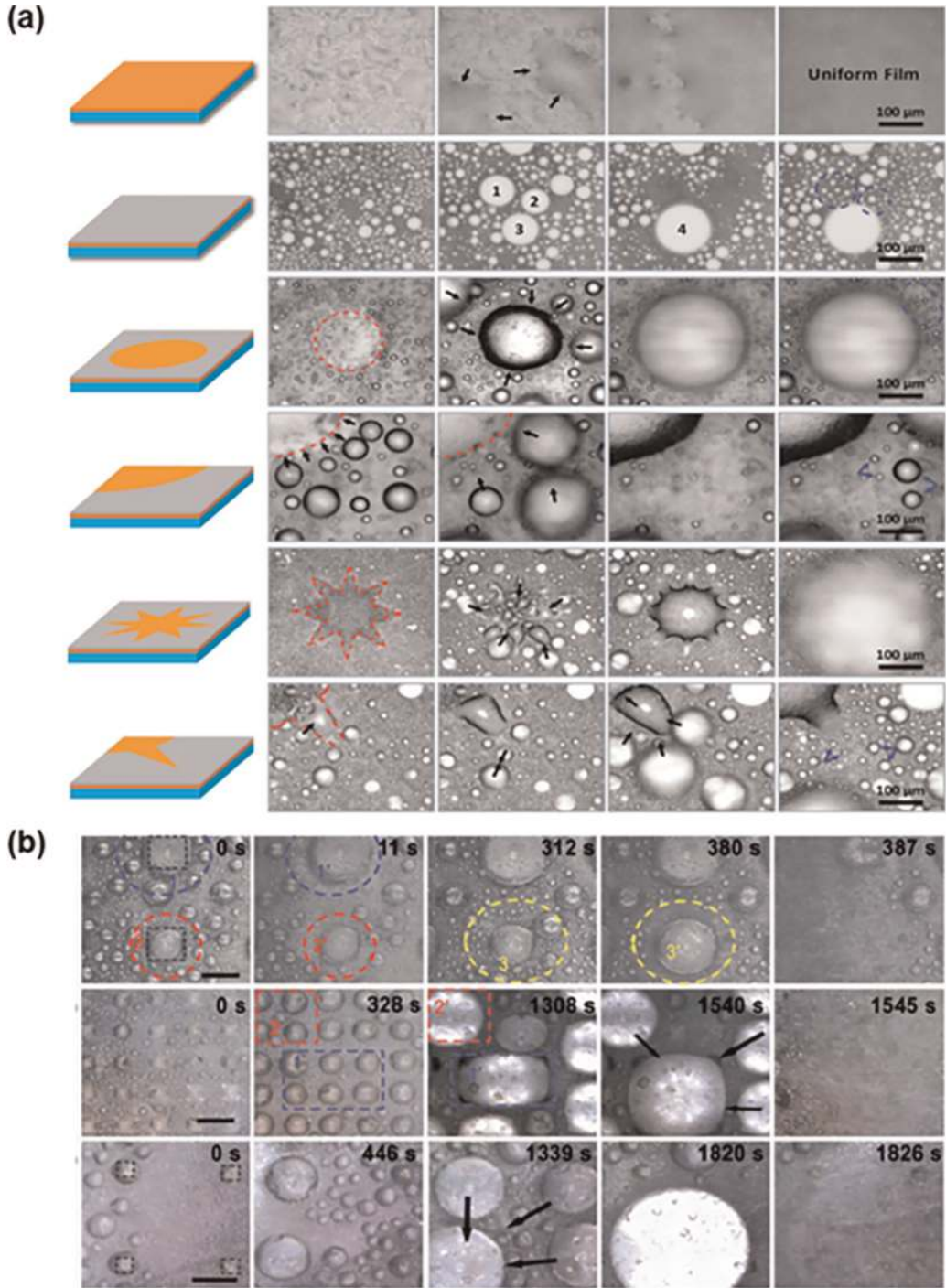


Figure 7. Water collection processes on various kinds of surfaces inspired by desert beetle. (a) Observation of water collecting behaviour on wettability-paradox surface with distinct graphic pattern (fabricated via FAS-modifying and UV selective photocatalytic decomposition): from top to bottom: superhydrophilic surface, superhydrophobic surface, circle-shaped pattern surface, circle-shaped edge surface, star-shaped edge surface, star-shaped circle surface [53], scale bar 100 μm. (b) Observation of water collecting behaviour on wettability-paradox surface with distinct arrangement density and size (fabricated via dopamine ink-jet printing), from top to bottom: superhydrophobic surface with 500/200/200 mm polydopamine patterns and respectively corresponding 1000/400/1000 mm separation [54], scale bar 500 μm.

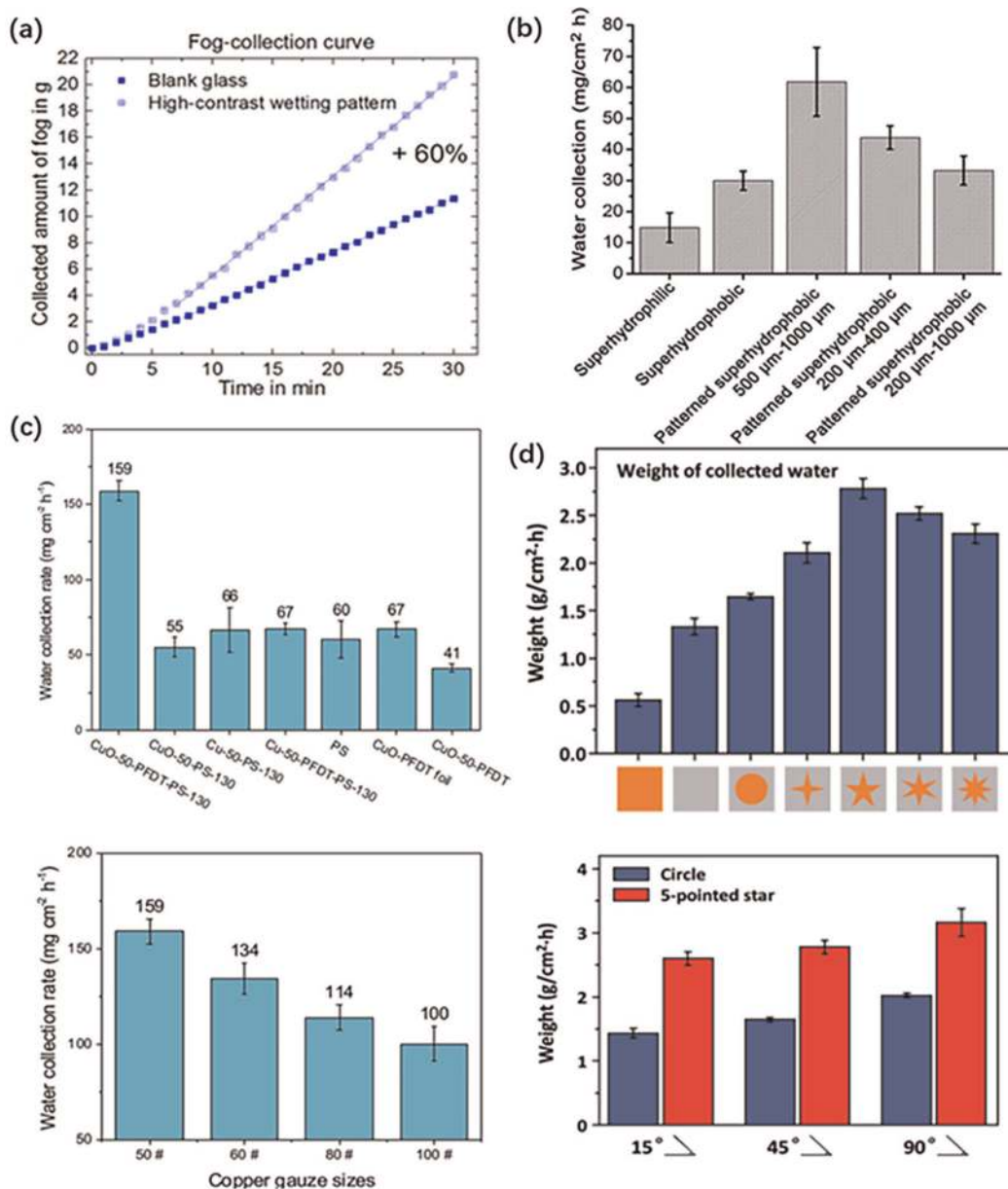


Figure 8. Distinct factors which may exert influences on fog-collecting efficiency of wettability-paradox surfaces inspired by desert beetle. (a) fog harvesting comparison of a piece of blank glass and a piece of glass with wettability-paradox surface [55]. (b) Influence of arrangement density and size on water collecting efficiency [54]. (c) Impacts of materials and density of composite on water collecting efficiency [52]. (d) Effects of pattern shapes and placed incline-angle upon fog-harvesting efficiency [53].

As composite can be made of different materials and density, how these factors affect water-collecting property had been investigated. As demonstrated in **Figure 8** (c), component and gauze size exert considerable influences on fog harvesting (due to the distinct contact degrees of the hydrophobic gauzes), where the maximum fog collecting rate was 1590 g/m²/h at ambient conditions (a simulated flow of fog about 0.12 m/s, relative humidity around the samples: 90–95% and temperature: 295 K, vertically placed) [52].

Fog harvesting performance is also linked to the graphic pattern on wettability paradox surface. Different fog-collecting processes was found on surfaces with various wettability features (**Figure 7a**). On uniformly superhydrophilic surface, the water droplet spread over surface while on total superhydrophobic surface, individual water droplets coalesced in disorder. However, water droplets gathered directionally toward the superhydrophilic place on bioinspired surfaces with wettability pattern. Diverse wettability pattern offers different route for water to combine and move away, resulting in distinct fog harvesting performance. Generally speaking, the fog collecting processes are relative continuous because immediately after a fog-water droplet move away, another one can be captured. Consequently, directional motion of tiny water droplets enhances the fog-collecting efficiency. In terms of fog-harvesting efficiency, the highest value occurred in 5-pointed star wettability pattern, which peaked at amazing $27,800 \text{ g/m}^2/\text{h}$ (fog flow 0.75 m/s in velocity under room temperature, inclined by 45° from the horizontal plane). In addition, the placed incline-angle also affects the collecting rate and simply by placing it vertically, the efficiency climbed to $\sim 32,000 \text{ g/m}^2/\text{h}$ (**Figure 8(d)**) [53].

5. Conclusion

In conclusion, fog-collecting function can be obtained by employing various biomimetic patterns inspired by diverse natural organisms. The water collection performance is firmly associated with the ability to seize fog-water from wet environment and the ability of directional droplet transport after the fog-water being captured. What on earth is more important may depend on the different foggy environment (e.g., the humidity or fog-flow rate of the environment). This question should be perfectly solved via simulated calculation and experimental verification in future research. Additionally, it is difficult to compare the absolute value of water-collecting efficiency since the fog-harvesting tests was carried out in different foggy environment (e.g., difficult humidity, fog-flow rate, temperature, and/or pressure) by researchers. However, the above sections have explained and concluded how to change the processing parameter to improve the water-collecting performance.

In terms of the raw materials of the fog harvester, both organic (including but not limited to various polymers and biomaterials) and inorganic (containing metals, glass, silicon slice, etc.) materials were employed. As for the wettability, appropriate hydrophilicity is beneficial to fog-water capturing while water transport can be accelerated using micro/nano-structured or/and hydrophobic surfaces.

Not only was the fog-harvesting efficiency significant, but also the mechanical property, durability, economy, degradability, and biocompatibility should be considered. It also merits noting that magnetic, light, electric, thermal, and pH responds of specific materials are possible to be designed as driving force for accelerating the speed of water direction removal, which would be a promising research direction in the future [2, 58].

The studies concerning bio-inspired fog-harvesting performance involves a multi-subject course. On the one hand, brand-new chemical, physical, and mechanical routes to manufacture pattern with fog-harvesting capacity has been developed. On the other hand, these findings are most likely to be put into practice in various domains such as fluidics, hydraulics, environment-protecting, pharmaceuticals, mechanics and textile.

Acknowledgements

Chang Li is supported by China Scholarship Council (No. 202008060076).

Conflict of interest

The authors declare no conflict of interest.

Author details

Chang Li^{1*}, Zhongshi Ni² and Ying Li³


1 Department of Mechanical Engineering, Imperial College London, London, UK

2 College of Engineering, University of Massachusetts Amherst, Amherst, MA, USA

3 School of Education, University of Glasgow, Glasgow, UK

*Address all correspondence to: c.li19@imperial.ac.uk; hamster@188.com

IntechOpen

© 2022 The Author(s). Licensee IntechOpen. This chapter is distributed under the terms of the Creative Commons Attribution License (<http://creativecommons.org/licenses/by/3.0>), which permits unrestricted use, distribution, and reproduction in any medium, provided the original work is properly cited. 

References

- [1] Li M, Li C, Blackman BRK, Saiz E. Energy conversion based on bio-inspired superwetting interfaces. *Matter*. 2021; **4**(11):3400-3414
- [2] Li M, Li C, Blackman BRK, Eduardo S. Mimicking nature to control bio-material surface wetting and adhesion. *International Materials Reviews*. 2022;**67**(6):658-681. DOI: 10.1080/09506608.2021.1995112
- [3] Seo D, Lee J, Lee C, Nam Y. The effects of surface wettability on the fog and dew fog-water harvesting performance on tubular surfaces. *Scientific Reports*. 2016;**6**:24276
- [4] Li C, Liu Y, Gao C, Li X, Xing Y, Zheng Y. Fog harvesting of a bioinspired nanocone-decorated 3D fiber network. *ACS Applied Materials & Interfaces*. 2019;**11**(4):4507-4513
- [5] Tsuchiya K, Ishii T, Masunaga H, Numata K. Spider dragline silk composite films doped with linear and telechelic polyalanine: Effect of polyalanine on the structure and mechanical properties. *Scientific Reports*. 2018;**8**:3654
- [6] Xiang P, Wang S, He M, Han Y, Zhou Z, Chen D, et al. The in vitro and in vivo biocompatibility evaluation of electrospun recombinant spider silk protein/PCL/gelatin for small caliber vascular tissue engineering scaffolds. *Colloids and Surfaces B-Biointerfaces*. 2018;**163**:19-28
- [7] Michalik M, Surmacka M, Stalmach M, Wilczek G, Kowalska T, Sajewicz M. Application of thin-layer chromatography to ecotoxicological study with the *steatoda grossa* spider web. *JPC-Journal of Planar Chromatography-Modern TLC*. 2018; **31**(1):7-12
- [8] Chen Y, Zheng Y. Bioinspired micro-/nanoscale fibers with a water collecting property. *Nanoscale*. 2014;**6**(14):7703-7714
- [9] Zheng Y, Bai H, Huang Z, Tian X, Nie F, Zhao Y, et al. Directional water collection on wetted spider silk. *Nature*. 2010;**463**(7281):640-643
- [10] Liu H, Cao G. Effectiveness of the Young-Laplace equation at nanoscale. *Scientific Reports*. 2016;**6**:23936
- [11] Feng S, Hou Y, Chen Y, Xue Y, Zheng Y, Jiang L. Water-assisted fabrication of porous bead-on-string fibers. *Journal of Materials Chemistry A*. 2013;**1**(29):8363-8366
- [12] Wang L, Ji X, Wang N, Wu J, Dong H, Du J, et al. Biaxial stress controlled three-dimensional helical cracks. *NPG Asia Materials*. 2012;**4**:e14
- [13] Xue Y, Chen Y, Wang T, Jiang L, Zheng Y. Directional size-triggered microdroplet target transport on gradient-step fibers. *Journal of Materials Chemistry A*. 2014;**2**(20):7156-7160
- [14] He X, Wang W, Liu Y, Jiang M, Wu F, Deng K, et al. Microfluidic fabrication of bio-inspired microfibers with controllable magnetic spindle-knots for 3d assembly and water collection. *ACS Applied Materials & Interfaces*. 2015;**7**(31):17471-17481
- [15] Tian Y, Zhu P, Tang X, Zhou C, Wang J, Kong T, et al. Large-scale water collection of bioinspired cavity-microfibers. *Nature Communications*. 2017;**8**:1080

- [16] Zhu H, Guo Z, Liu W. Biomimetic water-collecting materials inspired by nature. *Chemical Communications*. 2016;**52**(20):3863-3879
- [17] Bai H, Ju J, Sun R, Chen Y, Zheng Y, Jiang L. Controlled Fabrication and Water Collection Ability of Bioinspired Artificial Spider Silks. *Advanced Materials*. 2011;**23**(32):3708
- [18] Chen Y, Wang L, Xue Y, Jiang L, Zheng Y. Bioinspired tilt-angle fabricated structure gradient fibers: micro-drops fast transport in a long-distance. *Scientific Reports*. 2013;**3**:2927
- [19] Zhao L, Song C, Zhang M, Zheng Y. Bioinspired heterostructured bead-on-string fibers via controlling the wet-assembly of nanoparticles. *Chemical Communications*. 2014;**50**(73):10651-10654
- [20] Quere D, Dimeglio JM, Brochardwyart F. Spreading of liquids on highly curved surfaces. *Science*. 1990;**249**(4974):1256-1260
- [21] Bai H, Sun R, Ju J, Yao X, Zheng Y, Jiang L. Large-scale fabrication of bioinspired fibers for directional water collection. *Small*. 2011;**7**(24):3429-3433
- [22] Loscertales IG, Barrero A, Guerrero I, Cortijo R, Marquez M, Ganan-Calvo AM. Micro/nano encapsulation via electrified coaxial liquid jets. *Science*. 2002;**295**(5560):1695-1698
- [23] Sun ZC, Zussman E, Yarin AL, Wendorff JH, Greiner A. Compound core-shell polymer nanofibers by co-electrospinning. *Advanced Materials*. 2003;**15**(22):1929
- [24] Li D, McCann JT, Xia YN. Use of electrospinning to directly fabricate hollow nanofibers with functionalized inner and outer surfaces. *Small*. 2005;**1**(1):83-86
- [25] Song C, Zhao L, Zhou W, Zhang M, Zheng Y. Bioinspired wet-assembly fibers: From nanofragments to microhumps on string in mist. *Journal of Materials Chemistry A*. 2014;**2**(25):9465-9468
- [26] Zhang M, Zheng Y. Bioinspired structure materials to control water-collecting properties. *Materials Today-Proceedings*. 2016;**3**(2):696-702
- [27] Tian X, Bai H, Zheng Y, Jiang L. Bioinspired heterostructured bead-on-string fibers that respond to environmental wetting. *Advanced Functional Materials*. 2011;**21**(8):1398-1402
- [28] Dong H, Wang N, Wang L, Bai H, Wu J, Zheng Y, et al. Bioinspired electrospun knotted microfibers for fog harvesting. *ChemPhysChem*. 2012;**13**(5):1153-1156
- [29] Thakur N, Ranganath AS, Agarwal K, Baji A. Electrospun bead-on-string hierarchical fibers for fog harvesting application. *Macromolecular Materials and Engineering*. 2017;**302**(7):1700124
- [30] Ganesh VA, Ranganath AS, Baji A, Raut HK, Sahay R, Ramakrishna S. Hierarchical structured electrospun nanofibers for improved fog harvesting applications. *Macromolecular Materials and Engineering*. 2017;**302**(2):1600387
- [31] Du M, Zhao Y, Tian Y, Li K, Jiang L. Electrospun multiscale structured membrane for efficient water collection and directional transport. *Small*. 2016;**12**(8):1000-1005
- [32] Melin J, Quake SR. Microfluidic large-scale integration: The evolution of design rules for biological automation.

Annual Review of Biophysics and Biomolecular Structure. 2007;**36**:213-231

[33] Ji X, Guo S, Zeng C, Wang C, Zhang L. Continuous generation of alginate microfibers with spindle-knots by using a simple microfluidic device. RSC Advances. 2015;**5**(4):2517-2522

[34] Li X, Liu Y, Zhou H, Gao C, Li D, Hou Y, et al. Fog collection on a bio-inspired topological alloy net with micro-/nanostructures. ACS Applied Materials & Interfaces. 2020;**12**(4): 5065-5072

[35] Liu Y, Yang N, Li X, Li J, Pei W, Xu Y, et al. Water harvesting of bioinspired microfibers with rough spindle-knots from microfluidics. Small. 2020;**16**(9):1901819

[36] Zhong L, Zhu L, Li J, Pei W, Chen H, Wang S, et al. Recent advances in biomimetic fog harvesting: Focusing on higher efficiency and large-scale fabrication. Molecular Systems Design & Engineering. 2021;**6**(12):986-996

[37] Ju J, Bai H, Zheng Y, Zhao T, Fang R, Jiang L. A multi-structural and multi-functional integrated fog collection system in cactus. Nature Communications. 2012;**3**:1247

[38] Martorell C, Ezcurra E. The narrow-leaf syndrome: A functional and evolutionary approach to the form of fog-harvesting rosette plants. Oecologia. 2007;**151**(4):561-573

[39] Elbaum R, Zaltzman L, Burgert I, Fratzl P. The role of wheat awns in the seed dispersal unit. Science. 2007; **316**(5826):884-886

[40] Guo P, Zheng Y, Liu C, Ju J, Jiang L. Directional shedding-off of water on natural/bio-mimetic taper-ratchet array

surfaces. Soft Matter. 2012;**8**(6): 1770-1775

[41] Gursoy M, Harris MT, Carletto A, Yaprak AE, Karaman M, Badyal JPS. Bioinspired asymmetric-anisotropic (directional) fog harvesting based on the arid climate plant *Eremopyrum orientale*. Colloids and Surfaces A- Physicochemical and Engineering Aspects. 2017;**529**:959-965

[42] Gleiche M, Chi LF, Gedig E, Fuchs H. Anisotropic contact-angle hysteresis of chemically nanostructured surfaces. ChemPhysChem. 2001;**2**(3): 187-191

[43] Li D, Feng S, Xing Y, Deng S, Zhou H, Zheng Y. Directional bouncing of droplets on oblique two-tier conical structures. RSC Advances. 2017;**7**(57): 35771-35775

[44] Xu T, Lin Y, Zhang M, Shi W, Zheng Y. High-efficiency fog collector: Water unidirectional transport on heterogeneous rough conical wires. ACS Nano. 2016;**10**(12):10681-10688

[45] Xing Y, Wang S, Feng S, Shang W, Deng S, Wang L, et al. Controlled transportation of droplets and higher fog collection efficiency on a multi-scale and multi-gradient copper wire. RSC Advances. 2017;**7**(47):29606-29610

[46] Peng Y, He Y, Yang S, Ben S, Cao M, Li K, et al. Magnetically induced fog harvesting via flexible conical arrays. Advanced Functional Materials. 2015; **25**(37):5967-5971

[47] Dan L, Zheng Y. Self-propelled droplet movement on micro/nano anisotropic structures surface. Chemical Journal of Chinese Universities-Chinese. 2018;**39**(1):109-114

- [48] Parker AR, Lawrence CR. Water capture by a desert beetle. *Nature*. 2001; **414**(6859):33-34
- [49] White B, Sarkar A, Kietzig A. Fog-harvesting inspired by the *Stenocara* beetle-An analysis of drop collection and removal from biomimetic samples with wetting contrast. *Applied Surface Science*. 2013; **284**:826-836
- [50] Barthlott W, Schimmel T, Wiersch S, Koch K, Brede M, Barczewski M, et al. The salvinia paradox: Superhydrophobic surfaces with hydrophilic pins for air retention under water. *Advanced Materials*. 2010; **22**(21):2325-2328
- [51] Yang Y, Li X, Zheng X, Chen Z, Zhou Q, Chen Y. 3D-printed biomimetic super-hydrophobic structure for microdroplet manipulation and oil/water separation. *Advanced Materials*. 2018; **30**(9):1704912
- [52] Wang Y, Zhang L, Wu J, Hedhili MN, Wang P. A facile strategy for the fabrication of a bioinspired hydrophilic-superhydrophobic patterned surface for highly efficient fog-harvesting. *Journal of Materials Chemistry A*. 2015; **3**(37):18963-18969
- [53] Bai H, Wang L, Ju J, Sun R, Zheng Y, Jiang L. Efficient water collection on integrative bioinspired surfaces with star-shaped wettability patterns. *Advanced Materials*. 2014; **26**(29): 5025-5030
- [54] Zhang L, Wu J, Hedhili MN, Yang X, Wang P. Inkjet printing for direct micropatterning of a superhydrophobic surface: toward biomimetic fog harvesting surfaces. *Journal of Materials Chemistry A*. 2015; **3**(6):2844-2852
- [55] Lee DG, Lee D. Electro-mechanical properties of the carbon fabric composites with fibers exposed on the surface. *Composite Structures*. 2016; **140**: 77-83
- [56] Wu J, Zhang L, Wang Y, Wang P. Efficient and anisotropic fog harvesting on a hybrid and directional surface. *Advanced Materials Interfaces*. 2017; **4**(2):1600801
- [57] Yang X, Song J, Liu J, Liu X, Jin Z. A twice electrochemicaetching method to fabricate superhydrophobic-superhydrophilic patterns for biomimetic fog harvest. *Scientific Reports*. 2017; **7**:8816
- [58] Li C, Li M, Ni Z, Guan Q, Blackman BRK, Saiz E. Stimuli-responsive surfaces for switchable wettability and adhesion. *Journal of the Royal Society Interface*. 2021; **18**(179): 20210162